

How many Ultra High Energy Cosmic Rays could we expect from Centaurus A?

N. Fraija¹, M. M. González¹, M. Perez¹, A. Marinelli²

Instituto de Astronomía, UNAM, México, 04510

Instituto de Física, UNAM, México, 04510

nifraija@astro.unam.mx, magda@astro.unam.mx, jguillen@astro.unam.mx,
antonio.marinelli@fisica.unam.mx

Received _____; accepted _____

¹Instituto de Astronomía, Universidad Nacional Autónoma de México, Circuito Exterior, C.U., A. Postal 70-264, 04510 México D.F., México

²Instituto de Física, Universidad Nacional Autónoma de México, Circuito Exterior, C.U., A. Postal 70-264, 04510 México D.F., México

ABSTRACT

The Pierre Auger Observatory has associated a few ultra high energy cosmic rays with the direction of Centaurus A. This source has been deeply studied in radio, infrared, X-ray and γ -rays (MeV-TeV) because it is the nearest radio-loud active galactic nuclei. Its spectral energy distribution or spectrum shows two main peaks, the low energy peak, at an energy of 10^{-2} eV, and the high energy peak, at about 150 keV. There is also a faint very high energy ($E \geq 100$ GeV) γ -ray emission fully detected by the High Energy Stereoscopic System experiment. In this work we describe the entire spectrum, the two main peaks with a Synchrotron/Self-Synchrotron Compton model and, the Very High Energy emission with a hadronic model. We consider $p\gamma$ and pp interactions. For the $p\gamma$ interaction, we assume that the target photons are those produced at 150 keV in the leptonic processes. On the other hand, for the pp interaction we consider as targets the thermal particle densities in the lobes. Requiring a satisfactory description of the spectra at very high energies with $p\gamma$ interaction we obtain an excessive luminosity in ultra high energy cosmic rays (even exceeding the Eddington luminosity). However, when considering pp interaction to describe the γ -spectrum, the obtained number of ultra high energy cosmic rays are in agreement with Pierre Auger observations. Moreover, we calculate the possible neutrino signal from pp interactions on a Km^3 neutrino telescope using Monte Carlo simulations.

Subject headings: Galaxies: active – Galaxies: individual (Centaurus A) – High energy cosmic ray: UHECR — radiation mechanism: nonthermal

1. Introduction

Centaurus A (Cen A) is a Fanaroff & Riley Class I (FRI) active galactic nuclei (AGN). At a distance of 3.8 Mpc, it is the nearest radio-loud AGN and an excellent source for studying the physics of relativistic outflows and radio lobes. Its giant radio lobes, which subtend $\sim 10^\circ$ on the sky, are oriented primarily in the north-south direction. They were imaged at 4.8 GHz by the Parkes telescope (Junkes et al. 1993) and studied up to ~ 60 GHz by Hardcastle et al. 2009 utilizing the Wilkinson Microwave Anisotropy Probe (WMAP; Hinshaw et al. 2009). Cen A has a jet with an axis subtending an angle to the line of sight estimated as $15^\circ - 80^\circ$ (see, e.g. Horiuchi et al. 2006, and reference therein). Cen A has been well studied in radio, infrared, optical (Winkler et al. 1975; Mushotzky & Baity 1976; Bowyer et al. 1970; Baity et al. 1981), X-ray and γ -rays (MeV-TeV) (Hardcastle et al. 2003; Sreekumar et al. 1999; Aharonian et al. 2009). A tentative detection (4.5σ) of Cen A at very high energy (VHE) in the 1970s was reported by Grindlay et al. 1975. Subsequent VHE observations made with Mark III (Carramiñana et al. 1990), JANZOS (Allen 1993) and CANGAROO (Rowell et al. 1999; Kabuki et al. 2007) experiments resulted in flux upper limits. Cen A was also detected from MeV to GeV energies by all instruments on board of the Compton Gamma-Ray Observatory (CGRO) in the period of 1991-1995, revealing a peak in the spectral energy distribution (SED) in νF_ν representation at ~ 0.1 MeV with a maximum flux of about $\sim 10^{-9}$ erg cm $^{-2}$ s $^{-1}$ (Steinle et al. 1998). For more than 120 hr Cen A was observed (Aharonian et al. 2005, 2009) by High Energy Stereoscopic System (H.E.S.S.) experiment. A signal with a statistical significance of 5.0σ was detected from the region including the radio core and the inner kpc jets. The integral flux above an energy threshold of ~ 250 GeV was measured to be 0.8% of the Crab Nebula (apparent luminosity: $L(>250 \text{ GeV}) \sim 2.6 \times 10^{39}$ erg s $^{-1}$). The spectrum was described by a power law with a spectral index of $2.7 \pm 0.5_{stat} \pm 0.2_{sys}$. No significant flux variability was detected in the data set. Also, for a period of 10 months, Cen A was monitored by

Large Area Telescope (LAT) on board the Fermi Gamma-Ray Space Telescope. Flux levels were not significantly different from those found by the Energetic Gamma Ray Experiment Telescope (EGRET). However, the LAT spectrum was described with a photon index of $2.67 \pm 0.10_{stat} \pm 0.08_{sys}$ (Adbo et al. 2010). The spectra recorded by the cited gamma-ray experiments can be considered as the intrinsic spectra of Cen A because they are not affected by the Extragalactic Background Light (EBL) absorption.

It has been proposed that astrophysical sources accelerating ultra high energy cosmic rays (UHECRs) also could produce high energy γ -rays by proton interactions with photons at the source and/or the surrounding radiation and matter. Hence, VHE photons detected from Cen A could be the result of hadronic interactions of cosmic rays accelerated by the jet with photons radiated inside the jet or protons in the lobes (Gopal-Krishna et al. 2010; Rieger & Aharonian 2009; Kachelriess et al. 2009a,b; Romero et al. 1996; Isola et al. 2002; Honda 2009; Adbo et al. 2010; Dermer et al. 2009).

Pierre Auger Observatory (PAO) studied the spectra of UHECR above 57 EeV through their shower properties finding a mixed composition of p and Fe (Yamamoto et al. 2007; Abraham et al. 2008; Unger et al. 2007). By contrast, HiRes data are consistent with a dominant proton composition at those energies, but uncertainties in the shower properties (Unger et al. 2007) and in the particle physics extrapolated to this extreme energy scale (Engel et al. 2007) preclude definitive statements about the composition. At least two events of the UHECRs observed by PAO were detected (Abraham et al. 2007, 2008) inside of a 3.1° circle centered at Cen A.

Synchrotron/Synchrotron-Self Compton (SSC) models have been very successful in explaining the multiwavelength emission from Broad-Line Lacertae (BL Lac) objects (Bloom & Marscher 1996; Tavecchio et al. 1998). If FRIs are misaligned BL Lac objects, then one would expect synchrotron/SSC to explain their non-thermal spectral energy

distribution (SED) as well. In the synchrotron/SSC scenario the low energy emission, radio through optical, originates from synchrotron radiation while high energy emission, X-rays through VHE γ -rays, originates from SSC. However, many blazars have higher energy synchrotron peaks, so this mechanism then covers much of the X-ray band; for them only the γ -rays come from SSC mechanism. In Cen A, synchrotron/SSC model has been applied successfully to fit the two main peaks of the SED, jointly or separated, with one or more electron populations (Adbo et al. 2010; Chiaberge et al. 2001; Lenain et al. 2008; Orellana & Romero 2009; Hardcastle et al. 2009). On the other hand, some authors (Dermer et al. 2009; Gupta 2008; Becker & Biermann 2009) have considered hadronic processes to explain the VHE photons apparent in the SED.

In this work we use the fact that leptonic processes are insufficient to explain the entire spectrum of Cen A, and introduce hadronic processes that may leave a signature in the number of UHECRs observed on Earth. Our contribution is to describe jointly the SED of Cen A as well as the observed number of UHECR by PAO. We first require a description of the SED up to the highest energies obtaining parameters as: proton spectral index (α_p), proton proportionality constant (A_p) and the normalization energy (E_0). Then, we use these parameters to estimate the expected UHECRs observed by PAO. The main assumption here, is the continuation of the proton spectrum to ultra high energies. We also estimate the neutrino expectation in a hypothetical Km^3 telescope when considering that the VHE photons in the SED of Cen A are produced by pp interaction.

2. UHECRs from Cen A

The Pierre Auger Observatory, localized in the Mendoza Province of Argentina at $\approx 36^\circ$ S latitude, determines the arrival directions and energies of UHECRs using four fluorescence telescope arrays and 1600 surface detectors spaced 1.5 km. The large exposure

of its ground array, combined with accurate energy and arrival direction measurements, calibrated and verified from the hybrid operation with the fluorescence detectors, provides an opportunity to explore the spatial correlation between cosmic rays and their sources in the sky. The Pierre Auger Collaboration reported an anisotropy in the arrival direction of UHECRs (Abraham et al. 2007, 2008). While a possible correlation with nearby AGNs is still under discussion, it has been pointed out that some of the events can possibly be associated with Cen A (e.g. Gorbunov et al. 2008; Moskalenko et al. 2009; Kachelriess et al. 2009a).

The corrected PAO exposure for a point source is given by $\Xi t_{op} \omega(\delta_s)/\Omega_{60}$, where $\Xi t_{op} = (\frac{15}{4}) 9 \times 10^3 \text{ km}^2 \text{ yr}$, t_{op} is the total operational time (from 1st January 2004 until August 31st, 2007), $\omega(\delta_s) \simeq 0.64$ is an exposure correction factor for the declination of Cen A, and $\Omega_{60} \simeq \pi$ is the Auger acceptance solid angle (Cuoco & Hannestad 2008). For a proton power law with spectral index α_p and proportionality constant A_p , the expected number of UHECRs from Cen A observed by PAO above an energy, E_{min} , is given by,

$$N_{UHECR} = \frac{\Xi t_{op} \omega(\delta_s)}{(\alpha_p - 1) \Omega_{60}} A_p E_0 \left(\frac{E_{min}}{E_0} \right)^{-\alpha_p + 1} \quad (1)$$

where E_0 is the normalization energy. In other words, the expected number of UHECRs depends on the proton spectrum parameters. If we assume that protons at lower energies have hadronic interactions responsible for producing the observed gamma-ray spectra at very high energies then we can estimate these parameters. An interesting quantity is the apparent isotropic UHECR luminosity that also depends on the spectrum parameters as,

$$L_p = \frac{4 \pi d_z^2 A_p E_0^2}{(\alpha_p - 2)} \left(\frac{E_{min}}{E_0} \right)^{2 - \alpha_p} \quad (2)$$

where d_z is the distance to Cen A. On the other hand, during flaring intervals the apparent

isotropic jet power can reach $\approx 10^{46} \text{erg s}^{-1}$, hence the maximum particle energies of a cold relativistic wind with velocity β , apparent isotropic luminosity (L), Lorentz factor (Γ) and equipartition parameter of the magnetic field (ϵ_B) is given by (Dermer et al. 2009),

$$E_{max} \approx 3 \times 10^{20} \frac{\sqrt{\epsilon_B L / 10^{46} \text{ erg s}^{-1}}}{\beta^{3/2} \Gamma} \text{ eV} \quad (3)$$

where $\Gamma = 1/\sqrt{1 - \beta^2}$.

3. Leptonic Synchrotron/SSC Model

In accordance to the AGN model presented in detail by Becker & Biermann 2009, the synchrotron photons come from internal shocks in the jet. The associated electrons are accelerated by the first Fermi mechanism (Blandford & McKee 1976) and the non-thermal electron spectrum can be described by broken power-law given by,

$$\frac{dN_e}{dE_e} = A_e \begin{cases} \left(\frac{E_e}{E_0}\right)^{-\alpha} & E_{e,m} < E_e < E_{e,c} \\ \left(\frac{E_{e,c}}{E_0}\right)\left(\frac{E_e}{E_0}\right)^{-(\alpha+1)} & E_{e,c} \leq E_e < E_{e,Max} \end{cases} \quad (4)$$

where A_e is the proportionality electron constant, α is the electron spectral index, $E_{e,i} = \gamma_{e,i} m_e c^2$ and $\gamma_{e,i}$ is the electron Lorentz factor. The index i is m, c or Max for minimum, break and Maximum, respectively. For instance, $\gamma_{e,m}$ is the minimum electron Lorentz factor. $\gamma_{e,i}$ is given (Vietri 1995; Gallant 1999; Cheng & Wei 1996) as follows,

$$\begin{aligned} \gamma_{e,m} &= 1836.15 \frac{(\alpha - 2)}{(\alpha - 1)} \epsilon_e \Gamma \\ \gamma_{e,c} &= 548.48 (1 + z)^{-3} \frac{f_{es} \Gamma^2 \delta_D^3 \epsilon_B^{-1}}{\beta^2} \left(\frac{L^{obs}}{5 \times 10^{43} \text{ erg s}^{-1}} \right)^{-1} \left(\frac{dt^{obs}}{2.6 \times 10^6 \text{ s}} \right) \\ \gamma_{e,Max} &= 1.11 \times 10^8 (1 + z)^{-1} \frac{\delta_D \Gamma^{1/2} \epsilon_B^{-1/4}}{\beta} \left(\frac{L^{obs}}{5 \times 10^{43} \text{ erg s}^{-1}} \right)^{-1/4} \left(\frac{dt^{obs}}{2.6 \times 10^6 \text{ s}} \right)^{1/2} \end{aligned} \quad (5)$$

where ϵ_e is the electron energy shock, $\delta_D \equiv [\Gamma(1 - \beta\mu)]^{-1}$ is the Doppler factor, $\mu = \cos \theta$ is the observing angle along the line of sight, L^{obs} is the observed luminosity, dt^{obs} is the variability and f_{es} is the ratio of shell expansion time to synchrotron emission time given by (Bhattacharjee & Gupta 2003),

$$f_{es}(E_e) = \begin{cases} \frac{E_e}{E_{e,c}} & E_e < E_{e,c} \\ 1 & E_e \geq E_{e,c} \end{cases} . \quad (6)$$

The magnetic field, which comes from an equipartition law, is given by

$$B = 2.6 \text{ G } \epsilon_B^{1/2} \delta_D^{-2} \Gamma^{-1} \left(\frac{L^{obs}}{5 \times 10^{43} \text{ erg s}^{-1}} \right)^{-3/2} \left(\frac{dt^{obs}}{2.6 \times 10^6 \text{ s}} \right) \quad (7)$$

As the electrons are accelerated in the shock inside the magnetic field B , they emit photons by synchrotron radiation depending on the electron Lorentz factor. The photon energy in the source frame is related to the photon energy in the Earth's frame by $E_\gamma^{obs} = \frac{\delta_D}{1+z} E_\gamma$ (Dermer & Menon 2009) then, the observed energies (Rybicki & Lightman 1979) using equation 5 are given by,

$$\begin{aligned} E_{\gamma,m,syn}^{obs} &= 0.12 \text{ eV } \frac{(\alpha - 2)^2}{(\alpha - 1)^2} (1+z)^{-1} \delta_D^{-1} \Gamma \epsilon_e^2 \epsilon_B^{1/2} \left(\frac{L^{obs}}{5 \times 10^{43} \text{ erg s}^{-1}} \right)^{1/2} \left(\frac{dt^{obs}}{2.6 \times 10^6 \text{ s}} \right)^{-1} \\ E_{\gamma,c,syn}^{obs} &= 0.01 \text{ eV } (1+z)^{-5} \frac{f_{es}^2 \delta_D^5 \Gamma^3 \epsilon_B^{-3/2}}{\beta^4} \left(\frac{L^{obs}}{5 \times 10^{43} \text{ erg s}^{-1}} \right)^{-3/2} \left(\frac{dt^{obs}}{2.6 \times 10^6 \text{ s}} \right) \\ E_{\gamma,Max,syn}^{obs} &= 4.3 \times 10^8 \text{ eV } (1+z)^{-1} \frac{\delta_D}{\beta^2} \end{aligned} \quad (8)$$

We notice that the observed energies correspond to the cut-off energies in the synchrotron range and depend on parameters, as f_{es} and δ_D , that can be determined by fitting the first peak of the SED. On the other hand, the differential spectrum,

dN_γ/dE_γ , of the synchrotron photons is related to the electron spectrum through $f_{es}(E_e) E_e (dN_e/dE_e) dE_e = E_\gamma (dN_\gamma/dE_\gamma) dE_\gamma$, where $E_\gamma = C_e E_e^2$ and C_e is given in eq. (11). Thus, we can obtain the observed synchrotron spectrum as follow (Gupta & Zhang 2007)

$$\left(E_\gamma^2 \frac{dN_\gamma}{dE_\gamma}\right)_{syn}^{obs} = A_{e,\gamma} \begin{cases} \left(\frac{E_{\gamma,m,syn}}{E_0}\right)^{-4/3-(\alpha-3)} \left(\frac{E_{\gamma,c,syn}}{E_0}\right)^{-1/2} \left(\frac{E_{\gamma,syn}}{E_0}\right)^{4/3} & E_{\gamma,syn}^{obs} < E_{\gamma,m,syn}^{obs} \\ \left(\frac{E_{\gamma,c,syn}}{E_0}\right)^{-1/2} \left(\frac{E_{\gamma,syn}}{E_0}\right)^{-(\alpha-3)/2} & E_{\gamma,m,syn}^{obs} < E_{\gamma,syn}^{obs} < E_{\gamma,c,syn}^{obs} \\ \left(\frac{E_{\gamma,syn}}{E_0}\right)^{-(\alpha-2)/2} & E_{\gamma,c,syn}^{obs} < E_{\gamma,syn}^{obs} < E_{\gamma,Max,syn}^{obs} \end{cases} \quad (9)$$

where

$$A_{e,\gamma} = 2.16 \times 10^{-17} \frac{\Gamma^2 \delta_D^2 E_0^2 A_e e^{-\tau_{\gamma\gamma}}}{(1+z)^2} \left(\frac{dt^{obs}}{2.6 \times 10^6 s}\right)^2 \left(\frac{d_z}{3.8 \text{ Mpc}}\right)^{-2} (C_e E_0)^{\frac{\alpha-2}{2}} \quad (10)$$

$$C_e = 1.35 \times 10^{-19} (1+z)^2 \epsilon_B^{1/2} \delta_D^{-2} \Gamma^{-1} \left(\frac{L^{obs}}{5 \times 10^{43} \text{ erg s}^{-1}}\right)^{1/2} \left(\frac{dt^{obs}}{2.6 \times 10^6 s}\right)^{-1} eV^{-1} \quad (11)$$

and $\tau_{\gamma\gamma}$ is the optical depth (see fig. 3). Equation 9 represents the low energy contribution (IR to optical emission) to the whole spectrum.

To obtain the contribution from X-ray to γ -rays, we assume that the relativistic electrons inside the jet can upscatter the synchrotron photons in the same knot up to higher energies in accordance with,

$$E_{\gamma,m,SSC}^{obs} \sim \gamma_{e,m}^2 E_{\gamma,m,syn}^{obs}, \quad E_{\gamma,c,SSC}^{obs} \sim \gamma_{e,c}^2 E_{\gamma,c,syn}^{obs}, \quad E_{\gamma,Max,SSC}^{obs} \sim \gamma_{e,Max}^2 E_{\gamma,Max,syn}^{obs} \quad (12)$$

Now, with eqs. (5) and (8) we can finally obtain the inverse Compton photon energies,

$$E_{\gamma,m,SSC}^{obs} = 4.01 \times 10^5 \text{ eV} \frac{(\alpha-2)^4}{(\alpha-1)^4} (1+z)^{-1} \epsilon_e^4 \epsilon_B^{1/2} \Gamma^3 \delta_D^{-1} \left(\frac{L^{obs}}{5 \times 10^{43} \text{ erg s}^{-1}}\right)^{1/2} \left(\frac{dt^{obs}}{2.6 \times 10^6 s}\right)^{-1}$$

$$\begin{aligned}
E_{\gamma,c,SSC}^{obs} &= 3.19 \times 10^3 \text{ eV} (1+z)^{-11} (1+x)^{-4} \frac{f_{es}^4 \epsilon_e^{-7/2} \delta_D^{11} \Gamma^7}{\beta^3} \left(\frac{L^{obs}}{5 \times 10^{43} \text{ erg s}^{-1}} \right)^{-7/2} \left(\frac{dt^{obs}}{2.6 \times 10^6 \text{ s}} \right)^3 \\
E_{\gamma,max,SSC}^{obs} &= 5.4 \times 10^{24} \text{ eV} (1+z)^{-3} \frac{\epsilon_B^{-1/2} \delta_D^3 \Gamma}{\beta^4} \left(\frac{L^{obs}}{5 \times 10^{43} \text{ erg s}^{-1}} \right)^{-1/2} \left(\frac{dt^{obs}}{2.6 \times 10^6 \text{ s}} \right) \quad (13)
\end{aligned}$$

The Self Synchrotron Compton Spectrum is generally (Fragile et al. 2004) written as,

$$A_{ic} \left(\frac{dN_\gamma}{dE_\gamma} \right)_{SSC} = \frac{1}{E_{\gamma,IC}} \int \frac{dN_e}{dE_e} dE_e \int \left(\frac{dN_\gamma}{dE_\gamma} \right)_{syn} dE_\gamma \quad (14)$$

Combining Eqs. (9) and (4) with (14), we have that the observed Self-Synchrotron Compton spectrum is given by

$$\left(E_\gamma^2 \frac{dN_\gamma}{dE_\gamma} \right)_{SSC}^{obs} \simeq A_{\gamma,SSC} \begin{cases} \left(\frac{E_{\gamma,m,SSC}}{E_0} \right)^{-4/3-(\alpha-3)} \left(\frac{E_{\gamma,c,SSC}}{E_0} \right)^{-1/2} \left(\frac{E_{\gamma,SSC}}{E_0} \right)^{4/3} & E_{\gamma,SSC}^{obs} < E_{\gamma,m,SSC}^{obs} \\ \left(\frac{E_{\gamma,c,SSC}}{E_0} \right)^{-1/2} \left(\frac{E_{\gamma,SSC}}{E_0} \right)^{-(\alpha-3)/2} & E_{\gamma,m,SSC}^{obs} < E_{\gamma,SSC}^{obs} < E_{\gamma,c,SSC}^{obs} \\ \left(\frac{E_{\gamma,SSC}}{E_0} \right)^{-(\alpha-2)/2} & E_{\gamma,c,SSC}^{obs} < E_{\gamma,SSC}^{obs} < E_{\gamma,max,SSC}^{obs} \end{cases} \quad (15)$$

where,

$$\begin{aligned}
A_{\gamma,SSC} &= 2.32 \times 10^{-19} \frac{\Gamma^2 \delta_D^2 A_{ic}^{-1} A_e^2 E_0 e^{-\tau_{\gamma\gamma}}}{(1+z)^2} \left(\frac{dt^{obs}}{2.6 \times 10^6 \text{ s}} \right)^2 \left(\frac{d_z}{3.8 \text{ Mpc}} \right)^{-2} (C_e E_0)^{\frac{\alpha-2}{2}} \\
&\quad \left(\frac{0.505 \text{ MeV}}{E_0} \right)^{-(\alpha-1)} \left(\frac{E_{\gamma,c,syn}}{1 \text{ eV}} \right)^{-1/2} \left(\frac{E_{\gamma,ic}}{150 \text{ keV}} \right)^{-1/2} \quad (16)
\end{aligned}$$

Summarizing, the Leptonic model describes the whole spectrum at energies below a few tens of GeV as stated by equations 9 and 15 considering,

$$\left(E_\gamma^2 \frac{dN_\gamma}{dE_\gamma} \right)_{Lept\ model}^{obs} = \left(E_\gamma^2 \frac{dN_\gamma}{dE_\gamma} \right)_{syn}^{obs} + \left(E_\gamma^2 \frac{dN_\gamma}{dE_\gamma} \right)_{SSC}^{obs} \quad (17)$$

4. Hadronic Model

Some authors (Olinto 2000; Bhattacharjee & Sigl 1998; Stanev 2004; Dermer & Menon 2009) have considered possible different mechanisms where protons up to ultra high energies can be accelerated. Thus, we suppose that Cen A is capable of accelerating protons up to ultra high energies with a power law injection spectrum (Gupta 2008),

$$\frac{dN_p}{dE_p} = A_p E_p^{-\alpha_p} \quad (18)$$

where α_p is the proton spectral index and A_p is the proportionality constant. Energetic protons in the jet mainly lose energy by $p\gamma$ and pp interactions (Stecker 1968; Berezhinskii et al. 1990; Becker & Biermann 2009; Atoyan & Dermer 2003; Dermer & Menon 2009); as described in the following subsections.

4.1. $p\gamma$ interaction

The $p\gamma$ interaction takes place when accelerated protons collide with target photons. The single-pion production channels are $p + \gamma \rightarrow n + \pi^+$ and $p + \gamma \rightarrow p + \pi^0$, where the relevant pion decay chains are $\pi^0 \rightarrow 2\gamma$, $\pi^+ \rightarrow \mu^+ + \nu_\mu \rightarrow e^+ + \nu_e + \bar{\nu}_\mu + \nu_\mu$ and $\pi^- \rightarrow \mu^- + \bar{\nu}_\mu \rightarrow e^- + \bar{\nu}_e + \nu_\mu + \bar{\nu}_\mu$ (Atoyan & Dermer 2003).

In this analysis we suppose that protons interact with SSC photons (~ 150 keV) in the same knot. If so, the optical depth is given as $\tau_{p,ssc} \approx r_d \theta_{jet} \Gamma n_{\gamma,ssc}^{obs} \sigma_{p\gamma}$, where r_d is the value of the dissipation radius (Bhattacharjee & Gupta 2003), θ_{jet} is the jet aperture angle, $\sigma_{p\gamma} = 0.9$ mbarn is the cross section for the production of the delta-resonance in proton-photon interactions and $n_{\gamma,ssc}^{obs}$ is the particle density of SSC photons into the observer frame (Becker & Biermann 2009) given by,

$$n_{\gamma ssc}^{obs} \approx \frac{\epsilon_{knot} L^{obs}}{4\pi r_d^2 E_{\gamma,c}^{obs}} \quad (19)$$

Assuming that the luminosity of a knot along the jet is a fraction $\epsilon_{knot} \approx 0.1$ of the observed luminosity $L^{obs} = 5 \times 10^{43} \text{ erg s}^{-1}$ for $E_{\gamma,c}^{obs}$ keV, the optical depth is,

$$\tau_{p,ssc} \approx 8.2 \times 10^{-7} \Gamma^{-1} \left(\frac{\theta_{jet}}{0.3}\right) \left(\frac{\epsilon_{knot}}{0.1}\right) \left(\frac{L^{obs}}{5 \times 10^{43} \text{ erg s}^{-1}}\right) \left(\frac{r_d}{10^{16} \text{ cm}}\right)^{-1} \left(\frac{E_{\gamma,b}^{obs}}{150 \text{ keV}}\right)^{-1}. \quad (20)$$

The energy lost rate due to pion production is (Stecker 1968; Berezhinskii et al. 1990),

$$t'_{p,\gamma} = \frac{1}{2\gamma_p} \int_{\epsilon_0}^{\infty} d\epsilon \delta_{\pi}(\epsilon) \xi(\epsilon) \epsilon \int_{\epsilon/2\gamma_p}^{\infty} dx x^{-2} n(x) \quad (21)$$

where $n(x) = dn_{\gamma}/d\epsilon_{\gamma}(\epsilon_{\gamma} = x)$, $\sigma_{\pi}(\epsilon)$ is the cross section of pion production for a photon with energy ϵ in the proton rest frame, $\xi(\epsilon)$ is the average fraction of energy transferred to the pion, and $\epsilon_0 = 0.15$ is the threshold energy, $\gamma_p = \epsilon_p/m_p^2$.

The rate of energy loss, $t'_{p,\gamma}$, $f_{\pi^0,p\gamma} \approx t'_d/t'_{p,\gamma}$ (where $t'_d \sim r_d/\Gamma$ is the expansion time scale), can be calculated by following Waxman & Bahcall 1997 formalism.

$$f_{\pi^0,p\gamma} \approx \frac{(1+z)^2 L^{obs}}{8\pi\Gamma^2\delta_D^2 dt^{obs} E_{\gamma,b}^{obs}} \sigma_{\epsilon_{peak}} \xi(\epsilon_{peak}) \frac{\Delta\epsilon_{peak}}{\epsilon_{peak}} \begin{cases} \frac{E_p^{obs}}{E_{p,b}^{obs}} & E_p^{obs} < E_{p,b}^{obs} \\ 1 & E_p^{obs} \geq E_{p,b}^{obs} \end{cases} \quad (22)$$

Here, $\sigma_{peak} \approx 5 \times 10^{-28} \text{ cm}^2$ and $\xi(\epsilon_{peak}) \approx 0.2$ are the values of σ and ξ at $E_{\gamma} \approx \epsilon_{peak}$ and $\Delta\epsilon_{peak} \approx 0.2 \text{ GeV}$ is the peak width.

The differential spectrum, dN_{γ}/dE_{γ} of the photon-pions produced by $p\gamma$ interaction is related to the fraction of energy lost through the equation: $f_{\pi^0}(E_p) E_p dN_p/dE_p dE_p = E_{\gamma} dN_{\gamma}/dE_{\gamma} dE_{\gamma}$. If we take into account that π^0 typically carries 20% of the proton's

energy and that each produced photon shares the same energy then, we obtain the observed gamma spectrum through the following relationship,

$$\left(E^2 \frac{dN}{dE}\right)_{\pi^0-\gamma} = A_{p,\gamma} \begin{cases} \left(\frac{E_\gamma}{E_0}\right)^{-1} \left(\frac{E_{\gamma,c}}{E_0}\right)^{-\alpha_p+3} & E_\gamma < E_{\gamma,c} \\ \left(\frac{E_\gamma}{E_0}\right)^{-\alpha_p+2} & E_{\gamma,c} < E_\gamma \end{cases} \quad (23)$$

where

$$A_{p,\gamma} = 2.25 \times 10^{-13} \frac{\delta_D^{\alpha_p} E_0^2 A_p (11.1)^{2-\alpha_p} e^{-\tau_{\gamma\gamma}}}{(1+z)^\alpha} \left(\frac{E_{\gamma,c}^{obs}}{150 \text{ keV}}\right)^{-1} \left(\frac{L^{obs}}{5 \times 10^{43} \text{ erg s}^{-1}}\right) \left(\frac{dt^{obs}}{2.6 \times 10^6 \text{ s}}\right) \left(\frac{d_z}{3.8 \text{ Mpc}}\right)^{-2} \quad (24)$$

and

$$E_{\pi^0-\gamma,c}^{obs} = 212.49 \text{ GeV} \frac{\delta_D^2}{(1+z)^2} \left(\frac{E_{\gamma,b}^{obs}}{150 \text{ keV}}\right)^{-1} \quad (25)$$

The eq. 23 could represent the VHE photon contribution to the spectrum.

4.2. PP interaction

Hardcastle et al. 2009 argues that the number density of thermal particles within the giants lobes is $n_p \sim 10^{-4} \text{ cm}^{-3}$. If we assume that the accelerated protons collide with this thermal particle target then, the energy lost rate due to pion production is given by (Atoyan & Dermer 2003),

$$t'_{pp} = (n'_p k_{pp} \sigma_{pp})^{-1} \quad (26)$$

where $\sigma_{pp} = 30 \text{ mbarn}$ is the nuclear interaction cross section, $k_{pp} = 0.5$ is the inelasticity coefficient and n'_p is the comoving thermal particle density. The fraction of energy lost by pp is $f_{\pi^0,pp} \approx t'_d/t'_{pp}$ then,

$$f_{\pi^0,pp} = R n'_p k_{pp} \sigma_{pp} \quad (27)$$

where R is the distance to the lobes from the AGN core.

The differential spectrum, dN_γ/dE_γ of the photon-pions produced by pp interaction is related to the fraction of energy lost through the equation: $f_{\pi^0,pp}(E_p) E_p \left(\frac{dN_p}{dE_p}\right) dE_p = E_\gamma \left(\frac{dN_\gamma}{dE_\gamma}\right) dE_\gamma$. Taking into account that photon carries 18% of the proton energy, we have that the observed pp spectrum is given by (Gupta 2008),

$$\left(E^2 \frac{dN}{dE}\right)_{pp,\gamma} = A_{pp} \left(\frac{E_\gamma}{E_0}\right)^{2-\alpha_p} \quad (28)$$

where,

$$A_{pp} = 9.97 \times 10^{-21} \frac{\Gamma^2 \delta_D^2 E_0^2 A_p e^{-\tau_{\gamma\gamma}}}{(1+z)^2} \left(\frac{R}{100 \text{ kpc}}\right) \left(\frac{n'_p}{10^{-4} \text{ cm}^{-3}}\right) \left(\frac{dt^{obs}}{2.6 \times 10^6 \text{ s}}\right)^2 \left(\frac{d_z}{3.8 \text{ Mpc}}\right)^{-2} \quad (29)$$

The eq. 28 could represent the VHE photon contribution to the spectrum.

5. Calculation of physical parameters and expected UHECRs

A broadband fit to the SED of Cen A (data from Abdo et al. 2010) using our leptonic model (blue line) plus either $p\gamma$ or pp emission is shown in Figures 1 and 2 respectively. For this fit, we have adopted typical values reported in the literature such as luminosity (L^{obs}), variability (dt^{obs}), thermal particle target density (n_p) and lobes distance (R)(Abdo et al. 2010; Dermer et al. 2009; Hardcastle et al. 2009; Romero et al. 1996). The viewing angle was chosen in accordance with the observed infrared range (see, e.g. Horiuchi et al. 2006, and reference therein). Then, from the fit we obtain the values of the bulk Lorentz factor

(Γ), ratio of expansion time (f_{es}), proportionality constants (A_e , A_{ic} , $A_{p\gamma}/A_{pp}$), magnetic field parameter (ξ_B), electron parameters (ξ_e) and spectral index (α). Other quantities as magnetic field (B), electrons Lorentz factors ($\gamma_{e,min}$, $\gamma_{e,c}$), comoving radius (r_d), etc, are deduced these parameters. Table 1 shows all the values for used, obtained and deduced parameters in and from the fit.

The fit of the VHE photon spectrum with a hadronic model (either $p\gamma$ or pp interaction) determines the spectral index α_p , energy normalization E_0 and proportionality constant A_p (see section 2). So, we calculate the number of UHECRs expected on Earth. Results are given in Table 1. As shown, the expected number of UHECRs is extremely high if we consider the VHE spectral gamma contribution to come from $p\gamma$ interactions, while considering pp interactions the expected number of UHECRs is in agreement with PAO observations.

Name	Symbol	Value
Input parameters to the model		
Variability timescales (s)	dt^{obs}	2.5×10^6 (Adbo et al. 2010)
Luminosity (erg s^{-1})	L^{obs}	5×10^{43} (Adbo et al. 2010)
Jet angle (degrees)	θ	40 (Horiuchi et al. 2006)
Normalization constant (leptonic process) (MeV)	E_0	0.1 (Jourdain et al. 1993)
Normalization constant ($p\gamma$ process) (TeV)	E_0	1 (Aharonian et al. 2009)
Normalization constant (pp process) (TeV)	E_0	1 (Aharonian et al. 2009)
Thermal particle target density in lobes (cm^{-3})	n_p	1×10^4 (Hardcastle et al. 2009)
Lobes distance (kpc)	R	100 (Hardcastle et al. 2009)
Calculated parameters with the model		
Bulk Lorentz factor	Γ	2.06 ± 0.03
Electron spectral index	α	2.837 ± 0.004
Magnetic field parameter	ϵ_B	0.1073 ± 0.0008
Electron energy parameter	ϵ_e	0.79 ± 0.14
Ratio of expansion time	f_{es}	0.0385 ± 0.0003
Proportionality electron constant ($eV\text{cm}^2\text{s}$) $^{-1}$	A_e	$(4.368 \pm 0.003) \times 10^{15}$
Proportionality IC constant ($eV\text{cm}^2\text{s}$) $^{-1}$	A_{ic}	$(9.65 \pm 0.07) \times 10^{16}$
Proportionality proton constant ($TeV\text{cm}^2\text{s}$) $^{-1}$	A_{pp}	$(5.9 \pm 0.4) \times 10^{-7}$
Proportionality proton constant ($TeV\text{cm}^2\text{s}$) $^{-1}$	$A_{p\gamma}$	$(1.37 \pm 0.99) \times 10^4$
Proton spectral index	α_p	2.805 ± 0.008
Derived quantitatives		
Doppler factor	δ_d	1.47
Magnetic field (G)	B	0.19
Comoving radius (cm)	r_d	3.8×10^{16}
Minimum electron Lorentz factor	γ_m	1.36×10^3
Break electron Lorentz factor	γ_c	3.47×10^3
Apparent UHECR Luminosity ($p\gamma$) (erg s^{-1})	L_p	2.7×10^{49}
Apparent UHECR Luminosity (pp) (erg s^{-1})	L_p	2.9×10^{39}
Predicted number of events: $p\gamma$ interaction	$N_{ev,p\gamma}$	8.371×10^{10}
Predicted number of events: pp interaction	$N_{ev,pp}$	2.29

Table 1. Parameters used and obtained from and in the fit of the spectrum of Centaurus A.

6. Neutrino expectation for Cen A

The principal neutrino emission processes in the AGNs are hadronic. These interactions produce both, high energy neutrinos and high energy gamma rays, through pionic decay. As we mentioned before, hadronic interactions generate mainly pions by $p + p \rightarrow \pi^0 + \pi^+ + \pi^- + X$ (where X is an hadronic product) and $p + \gamma \rightarrow \Delta^+ \rightarrow \pi^0 + \pi^+$. The resulting neutral pion decays into two gamma rays, $\pi_0 \rightarrow \gamma\gamma$, and the charged pion into leptons and neutrinos, $\pi^\pm \rightarrow e^\pm + \nu_\mu/\bar{\nu}_\mu + \bar{\nu}_\mu/\nu_\mu + \nu_e/\bar{\nu}_e$. The effect of neutrino oscillations on the expected flux balances the number of neutrinos per flavor (Becker 2008) arriving at Earth. Therefore, the measured emission of high energy gamma rays from AGNs suggests the possibility to have an equivalent high-energy neutrino flux. In the case of Cen A the redshift is $z = 0.0018$, therefore VHE photons are not absorbed from EBL and we can consider the observed high energy gamma ray spectra as the intrinsic spectra emitted by this source and we can use it for the neutrino flux estimation.

Concerning the physics environment of Cen A, the optimistic conditions assumed to calculate the neutrino expectations are the following,

1. The high energy gamma ray flux detected by HESS are produced according to the pp hadronic scenario in Cen A.
2. The considered neutrino flux correlated to high energy gamma ray activity has a minimum duration of 1 year (i.e. the source is assumed to be stable).
3. The neutrino spectrum of Cen A is assumed without any cut-off.
4. The observed gamma-ray spectrum is considered as the intrinsic spectrum of Cen A.

Considering that neutrinos and gamma rays are produced by the same hadronic interaction (pp), we follow the description of Becker(2008) to correlate these two messengers

and we assume the neutrino spectrum to be the same as the VHE gamma spectrum recorded by H.E.S.S. Therefore we perform a Monte Carlo simulation of a possible Km^3 neutrino telescope in the Mediterranean sea in order to calculate the expected neutrino event rate. We choose this location to have a good sensitivity with respect to the position of Cen A.

The Monte Carlo simulation takes into account the neutrino source position, the propagation of neutrino through water, the charged current interaction with the respective muon production, the Cherenkov light produced by the muon, the photons produced by the electromagnetic showers and the response of the simulated neutrino telescope. Then we calculate the signal to noise ratio in the telescope.

In this analysis the neutrino “backgrounds” are represented by atmospheric neutrinos and cosmic diffuse neutrinos. The atmospheric neutrino “background” is generated by the interaction of high energy cosmic rays with nuclei in the atmosphere. The cosmic diffuse neutrino “background” is taken as the average rate of neutrinos generated by all the galactic and extragalactic non-resolved sources. This cosmic diffuse neutrino flux is discussed by Waxman and Bahcall (Bahcall & Waxman 2001; Waxman & Bahcall 1998) and his upper limit is given as $E_\nu^2 d\Phi/dE_\nu < 4.5 \times 10^{-8} \text{GeVcm}^{-2}\text{s}^{-1}\text{sr}^{-1}$. The atmospheric neutrino flux implemented in our Monte Carlo is well described by the Bartol model (Barr et al. 2004, 2006) in the range between 10 GeV and 100 TeV. We do not consider the “background” from atmospheric muon flux since it is filtered out by the Earth because Cen A is most of the time under the horizon for our hypothetical telescope, see Fig.5. For the calculation of signal to noise ratio we take into account only the “background” inside the portion of the sky covered by a cone centered in the Cen A position and having an opening angle of 1° . This selection is motivated by the angular resolution of our neutrino telescope.

Using the assumed neutrino spectrum we obtain for the Km^3 telescope the expected neutrino event rate shown in Fig. 4. As observed, the integrated signal neutrino event rate

in one year of recording data is one order of magnitude below the cosmic neutrino event rate and two order of magnitude below the atmospheric neutrino event rate reconstructed in the region around Cen A. Moreover, even considering few years of neutrino telescope operation, with the considered spectrum, we are not able to disentangle neutrino emission from Cen A.

7. Summary and conclusions

We have presented a leptonic and hadronic model to describe the broadband photon spectrum of Cen A. Our model has eight free parameters (equipartition magnetic field, equipartition electron energy, bulk Lorentz factor, spectral index, ratio of expansion time and proportionality constants). The leptonic model describes the spectrum up to a few GeV energies while the hadronic model describes the Cen A spectrum at TeV energies. Two hadronic interactions have been considered, $p\gamma$ and pp interactions. In the first case, the target is considered as SSC photons with energy of ~ 150 keV, while in the second case, the target protons are those in the lobes of Cen A. Only one hadronic interaction is considered at the time but in both cases, the proton spectrum is extrapolated up to ultra high energies to estimate the number of UHECR events expected at Earth. We have required a good description of the photon spectrum to obtain values for the quantities required to estimate the UHECR events.

When $p\gamma$ interaction is considered, the expected number of UHECR obtained is several orders of magnitude above the observed by PAO. However, when pp interaction is considered, the expected number of UHECR is in very good agreement with PAO observations.

We have also calculated the neutrino event rate from pp interactions observed by a

hypothetical Km^3 neutrino telescope in the Mediterranean sea. We have calculated the signal to noise ratio considering atmospheric and cosmic neutrino “backgrounds”. We have obtained that the expected signal event rate is below the required one to disentangle the neutrino emission from Cen A from the ”backgrounds”.

We thank the anonymous referee for the comments given to improve the paper. We also thank to Charles Dermer, Markus Bötcher, Parisa Roustazadeh, Bin Zhang, Giulia DeBonis, Bachir Bouhadeh, Mauro Morganti, Dario Grasso, Antonio Stamerra and Teresa Montaruli for useful discussions.

This work was supported by DGAPA-UNAM (Mexico) Project Numbers IN112910 and IN105211 and Conacyt project number 105033.

REFERENCES

- Abraham J. et al. (Pierre Auger Collaboration), 2007, *Science*, 318, 938
- Abraham J. et al. (Pierre Auger Collaboration), 2008, *ApJ*, 29, 198.
- Abdo A. A. et al. (FERMI Collaboration), 2010, *ApJ*, 719, 1433.
- Aharonian F. et al. (HESS Collaboration), 2005, *A&A*, 441, 465.
- Aharonian F. et al. (HESS Collaboration), 2009, *ApJ*, 695, L40.
- Allen W.H. et al. (JANZOS Collaboration), 1993, *ApJ*, 405, 554.
- Atoyan A. M & Dermer C. D., 2003, *ApJ*, 589, 79.
- Baity W. A. et al., 1981, *ApJ*244, 429.
- Bahcall J. & Waxman E., 2001, *Physical Review D.*, 64(2): 023002.
- Barr G.D., Gaisser T. K. , Lipari P., Robbins S. & Stanev T., *Phys. Rev. D* 70, 023006 (2004).
- Barr G.D., Gaisser T. K., Robbins S., & Stanev T., *Phys. Rev. D* 74, 094009 (2006).
- Becker J. K., 2008, *Physics Reports*, 458 , 173.
- Becker J. K. & Biermann P. L., 2009, *Astropart. Phys.* 31, 138.
- Berezinskii, V.S., Bulanov S. V., Dogiel V. A., Ginzburg V. I. & Ptuskin V. S. 1990, *Astrophysics of Cosmic Rays* (North-Holland:Amsterdam), Ch. 4.
- Bhattacharjee P. & Gupta N., 2003, *Astropart. Phys.*, 20, 169.
- Bhattacharjee P. & Sigl G., 2000, *Phys. Rept.*, 327, 109.

- Blandford R. D. & McKee C. F., 1976, *Phys. Fluids*. 19, 1130.
- Bloom, S. D. & Marscher, A. P. 1996, *ApJ*, 461, 657.
- Bowyer C. S., Lampton M., Mack J. & De Mendonca F., 1970, *ApJ*161 L1.
- Carramiñana et al., 1990, *A&A*, 228, 327.
- Cheng K. S. & Wei D. M. 1996, *MNRAS*, 283, L133.
- Chiaberge M., Capetti A. & Celotti 2001, *MNRAS*, 324, L33.
- Cuoco A. & Hannestad S., 2008, *Phys. Rev. D*, 78, 023007.
- Dermer C. D., Razzaque S., Finke J. D. & Atoyan A., 2009, *New J. Phys.* 11, 065016.
- Dermer C. D. & Menon G. 2009, *High energy radiation from Black Holes*, Princeton University Press. 2009.
- Engel R.l R (The Pierre Auger Collaboration), 2007, arXiv: 0706.1921.
- Fragile P. C., Mathews G., Poirier J. & Totani T., 2004, *Astropart. Phys.* 20, 591.
- Gallant Y. A., 2002, *Lectures Notes in Physics*, 589, 24.
- Gopal-Krishna, Biermann P. L. , De Souza V. & Wiitta P. J., 2010, *Astropart. Phys.* 720, L155.
- Gorbunov D., Tinyakov, P. Tkachev, I & Troitsky, S., 2008, *Sov. J. Exp. Theor. Phys. Lett*, 87, 461.
- Grindlay J. E, Helmken H. F., Brown R. H., Davis, J. & Allen L. R., 1975, *ApJ*, 197, L9.
- Gupta N. & Zhang B. 2007, *MNRAS*, 380, 78.
- Gupta N., 2008, *JCAP*, 7060806, 022.

- Hague J. D.,(Pierre Auger Collaboration), 2009, Proc. 31st ICRC, Lodz
- Hardcastle M. J., Worrall D. M., Kraft R. P., Forman W. R., Jones C. & Murray S. S.,
2003, ApJ, 593, 169.
- Hardcastle M. J., Cheung C. C., Feain I. J. & Stawarz L., 2009, MNRAS, 393, 1041.
- Hinshaw et al., 2009, ApJS, 180, 225.
- Honda M., 2009, ApJ, 706, 1517.
- Horiuchi S., Meier D. L., Preston R. A. & Tingay S. J., 2006, PASJ, 58, 211.
- Isola, C., Lemoine M. & Sigl G., 2002, Phys. Rev. D, 65, 023004.
- Junkes E. et al., 1993, ApJ, 412, 586.
- Junkes N., Haynes, R. F., Harnett, J.I., & Jauncy, D. L. 1993, A&A, 269,29.
- Kabuki, S. et al. (CANGAROO III Colaboration) 2007, ApJ, 668, 968.
- Kachelriess M., Ostapchenko S. & Tomas R., 2009, New J. Phys. 11, 065017.
- Kachelriess M., Ostapchenko S. & Tomas R., 2009, Int. J. Mod. Phys. D 18, 1591.
- Lenain J. P., Boisson C., Sol H. & Katarzynski K., 2008 A&A478, 111.
- Moskalenko, I. V., Stawarz, L., Porter T. A. & Cheung, C. C., 2009, ApJ, 693, 1261.
- Mushotzky R. F., Baity W. A., Wheaton W.A., & Peterson L. E., 1976 , ApJ, 206, L45.
- Olinto A. V., 2000, Phys. Rept. 333, 329.
- Orellana M. & Romero G. E., 2009 AIP Conf. Proc., 1123, 242.
- Raue M. & Mazin D. , 2008, International Journal of Modern Physics 17, 1515.

- Rieger F. M. & Aharonian F. A., 2009, *A&A*, 506, L41.
- Romero G. E., Combi J. A., Anchordoqui L.A. & Perez S. E., 2009, *Astropart. Phys.*, 5, 279.
- Rowell, G. P. et al. (CANGAROO III Colaboration) 1999, *Astropart. Phys.* 11, 217.
- Rybicki G.B. & Lightman A.P.1979, *Radiative processes in Astrophysics* (Wiley, New York. 1979).
- Sreekumar P., Bertsch D. L., Hartman R. C., Nolan P.L. & Thompson D. J., 1999, *ApJ*, 11, 221.
- Stanev T., 2004, *High Energy Cosmic Rays*, Springer, 2004.
- Stecker F. W. 1968, *Phys. Rev. Lett.*, 21, 1016.
- Steinle H. et al., 1998, *A&A*, 330, 97.
- Tavecchio, F., Maraschi, L. & Ghisellini, G., 1998, *ApJ*, 509, 608.
- Unger M., Engel R., Schussler F., Ulrich R. & Pierre Auger Collaboration, 2007, *Astron. Nachrichten*, 328, 614.
- Unger M., Dawson B.R., Engel R., Schussler F. & Ulrich R., 2008, *Nucl. Instrum. Methods Phys. Res. A*, 588, 433.
- Vietri M., 1995 *ApJ*, 453, 883.
- Waxman E. & Bahcall J., 1997, *Phys. Rev. Lett.* 78, 12.
- Waxman E. & Bahcall J., 1998, *Texas simposium on Relativistic Astrophysics and Cosmology*, December 1998.
- Winkler F. P. & White A. E. 1975 *ApJ*, 199, L139.

Yamamoto T. & Pierre Auger Collaboration, 2007, arXiv:0707.2638.

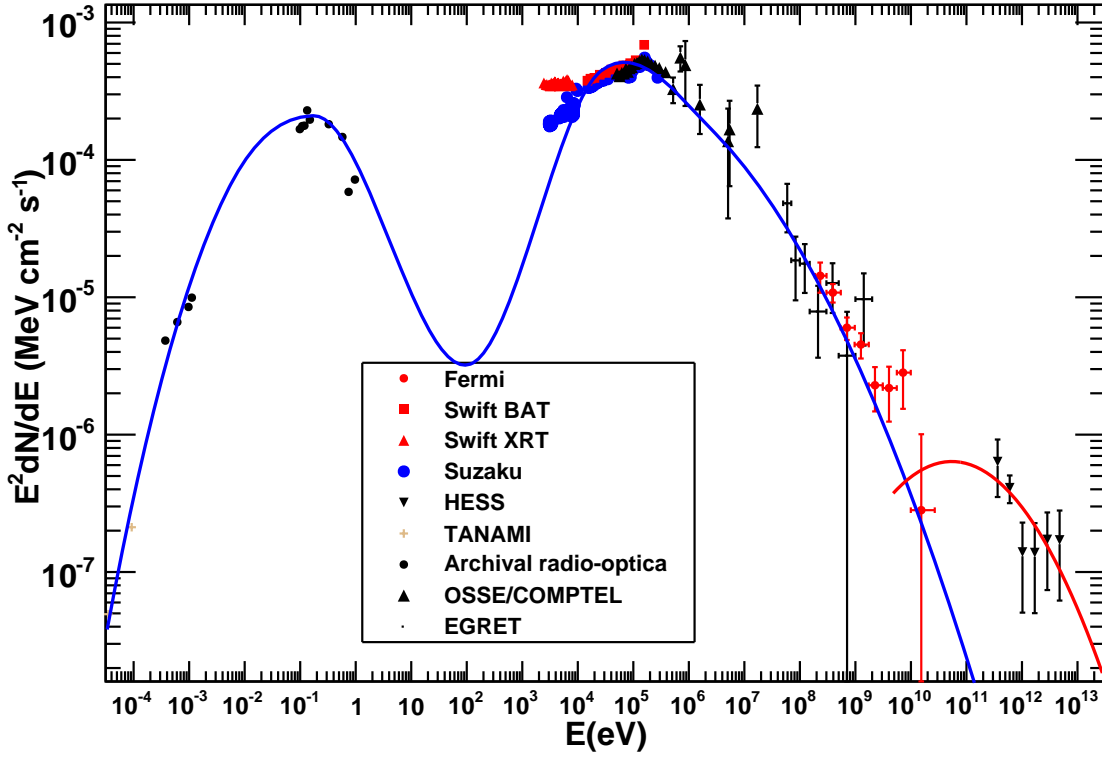


Fig. 1.— Fit of observed spectral energy distribution (SED) of Cen A. The blue line is a fit to the broadband SED using the leptonic model described in section 2, while the red curve is the $p\gamma$ contribution described in section 3.

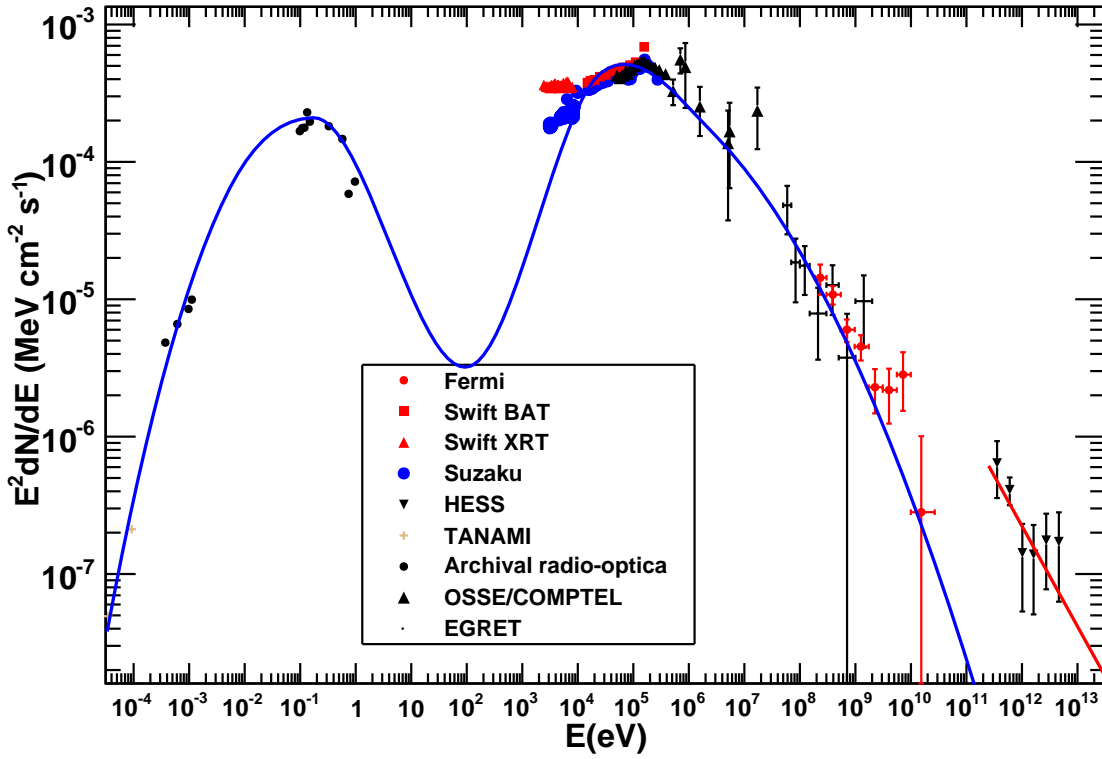


Fig. 2.— Fit of observed spectral energy distribution (SED) of Cen A. The blue line is a fit to the broadband SED using the leptonic model described in section 2, while the red curve is the pp contribution described in section 3.

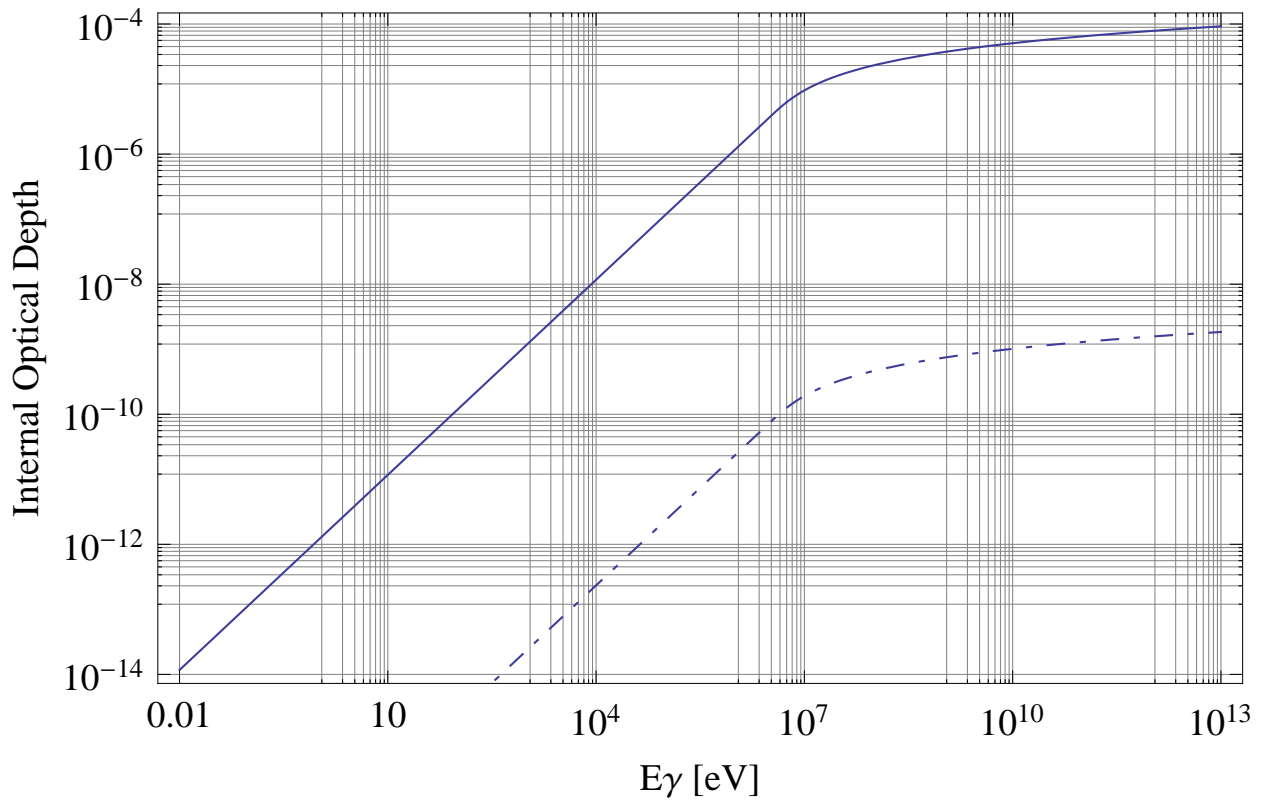


Fig. 3.— Internal optical depth $\tau_{\gamma\gamma}$ as a function of photon energy E_γ for two different luminosities: $L^{obs} = 5.0 \times 10^{43}$ erg/s (solid line) and $L^{obs} = 1.0 \times 10^{39}$ erg/s (dot-dashed line)

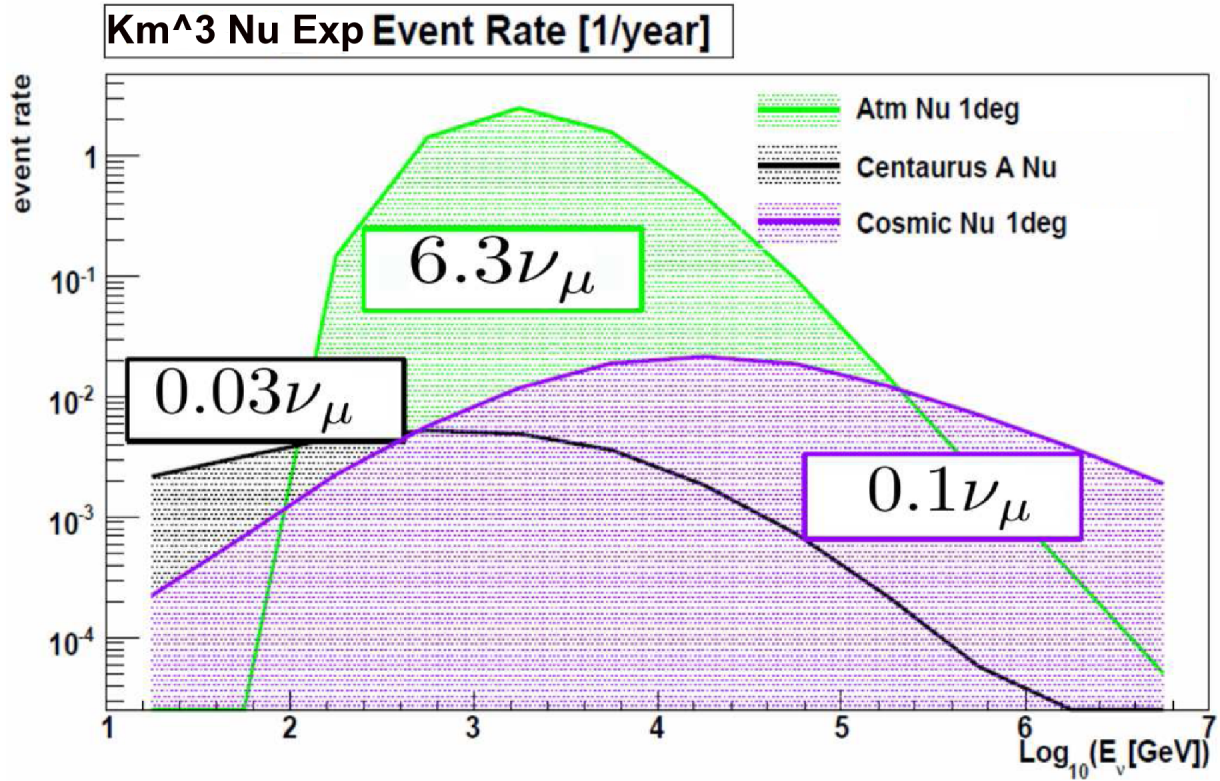


Fig. 4.— Neutrino event rate as a function of neutrino energy. The expected Centaurus A event rate for one year of observation with a Km^3 neutrino telescope assuming the spectrum measured by HESS (black line), the event rate for atmospheric neutrinos (green line) and cosmic neutrinos (purple line) considering the solid angle of 1° around the sources. A quality cut has been applied to reconstructed events. The integrated number of neutrinos is given for each case.

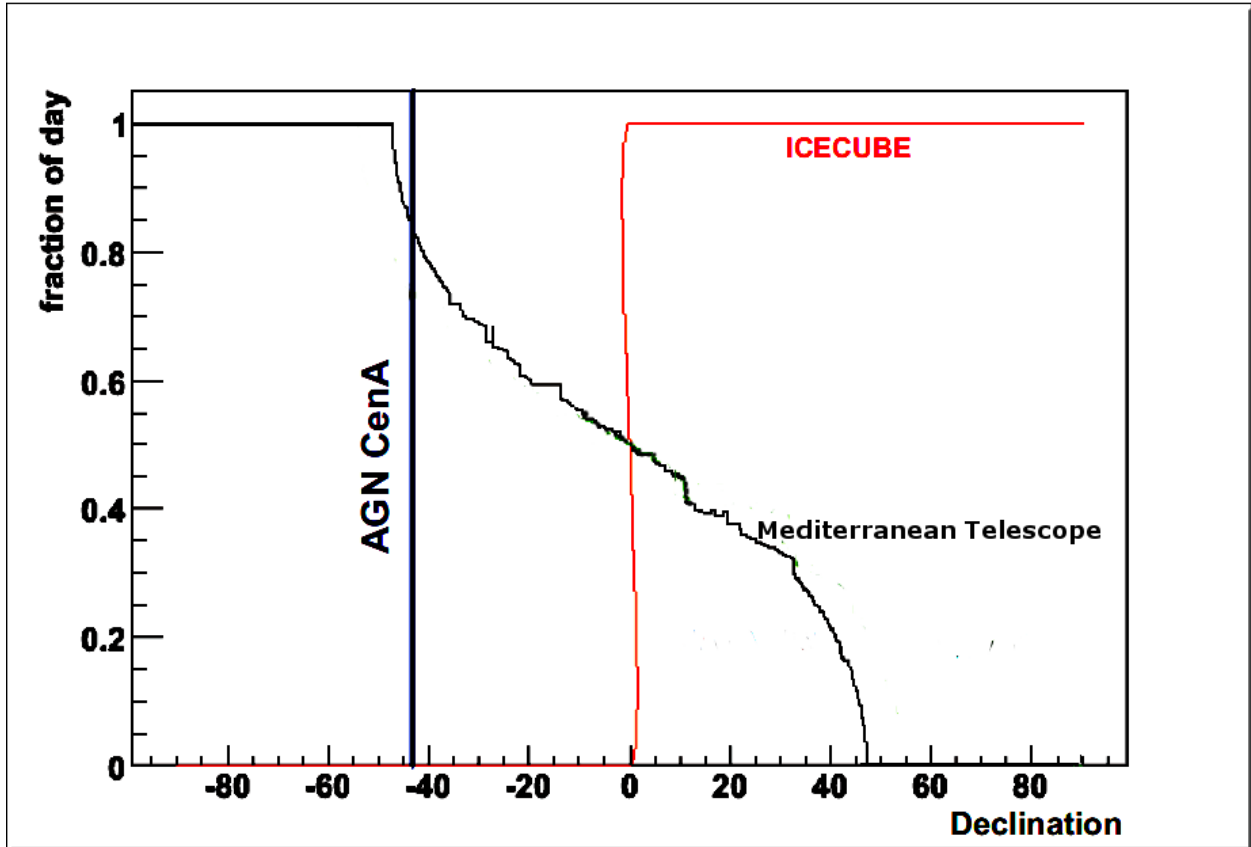


Fig. 5.— Calculated the Fraction of Day (FoD) when a source with a given declination is below the horizon with respect to our hypothetical Km³ Telescope (solid line) in the Mediterranean and ICECUBE experiments (dashed line). For Cen A, FoD is ≈ 0.8 when Km³ Telescope is considered. For ICECUBE, Cen A is all the time above the horizon.